HHS Public Access

Author manuscript

Neuroscience. Author manuscript; available in PMC 2016 September 24.

Published in final edited form as:

Neuroscience. 2015 September 24; 304: 146–160. doi:10.1016/j.neuroscience.2015.07.056.

BDNF over-expression increases olfactory bulb granule cell dendritic spine density in vivo

Brittnee McDole, **Ceylan Isgor**, **Christopher Pare**, and **Kathleen Guthrie***

Department of Biomedical Science, Charles E. Schmidt College of Medicine, Florida Atlantic University

Abstract

Olfactory bulb granule cells are axon-less, inhibitory interneurons that regulate the activity of the excitatory output neurons, the mitral and tufted cells, through reciprocal dendrodendritic synapses located on granule cell spines. These contacts are established in the distal apical dendritic compartment, while granule cell basal dendrites and more proximal apical segments bear spines that receive glutamatergic inputs from the olfactory cortices. This synaptic connectivity is vital to olfactory circuit function and is remodeled during development, and in response to changes in sensory activity and lifelong granule cell neurogenesis. Manipulations that alter levels of the neurotrophin brain-derived neurotrophic factor (BDNF) in vivo have significant effects on dendritic spine morphology, maintenance and activity-dependent plasticity for a variety of CNS neurons, yet little is known regarding BDNF effects on bulb granule cell spine maturation or maintenance. Here we show that, in vivo, sustained bulbar over-expression of BDNF produces a marked increase in granule cell spine density that includes an increase in mature spines on their apical dendrites. Morphometric analysis demonstrated that changes in spine density were most notable in the distal and proximal apical domains, indicating that multiple excitatory inputs are potentially modified by BDNF. Our results indicate that increased levels of endogenous BDNF can promote the maturation and/or maintenance of dendritic spines on granule cells, suggesting a role for this factor in modulating granule cell functional connectivity within adult olfactory circuitry.

*Corresponding author: Kathleen Guthrie, Ph.D., Dept. of Biomedical Science, BC 208, Charles E. Schmidt College of Medicine, Florida Atlantic University, 777 Glades Road, Boca Raton, FL, 33431, Phone: 561-297-0457, FAX: 561-297-2221, kguthrie@health.fau.edu.

Conflict of Interest

The authors state there are no known conflicts of interest related to the publication of this work, financial or otherwise.

Author Contributions

All authors have approved the final manuscript reporting this work. KG conceived and planned the experiments. BM performed mouse genotyping, ELISAs, Western blotting experiments, cell reconstructions, and morphometric analyses. CI performed Golgi-Cox tissue processing and assisted with reconstructions and morphometric analyses. CP performed in situ hybridization and quantitative densitometry. KG, CI, and BM participated in analysis and interpretation of data, including statistics. KG and BM wrote the manuscript and made the figures.

Keywords

brain-derived neurotrophic factor; TrkB; dendrite morphology; dendrodendritic; spine maintenance; GABAergic neurons

Introduction

Granule cells (GCs) of the main olfactory bulb are a large population of γ-aminobutyric acid (GABA)-synthesizing interneurons that lack axons and mediate inhibition of the principal excitatory output neurons, the mitral and tufted cells (MTCs). These output neurons extend lateral dendrites in the external plexiform layer (EPL) that are contacted by pedunculated, headed spines (aka, gemmules) arising from GC distal apical dendrites, and at these contacts, reciprocal dendrodendritic synapses are established (Mori et al., 1999; Shepherd, 2004; Nagayama et al., 2014). Glutamate released from MTC dendrites activates granule cells, triggering NMDA receptor- and Ca^{+2}-dependent dendritic release of GABA onto the MTC dendrites (Chen et al., 2000; Shepherd et al., 2007; Urban and Arevian, 2009). This in turn mediates feedback inhibition, as well as lateral inhibition of other, nearby MTCs with lateral dendrites that also are contacted by the stimulated granule cells, and (Egger and Urban, 2006; Shepherd et al., 2007; Urban and Arevian, 2009; Bywalez et al., 2015). This synaptic connectivity is vital to the processing and encoding of odor information that is then relayed to higher olfactory areas in forebrain including the piriform cortex (Price, 1973; Scott et al., 1980; Shepherd, 2004). Changes in this functional synaptic organization has significant consequences for odor processing and olfactory-mediated behaviors (Abraham et al., 2010; Diaz et al., 2012; Mizuguchi et al., 2012).

Dendritic spines are highly plastic structures, capable of undergoing adaptive morphological and physiological changes, both during development and in adulthood, in response to a wide range of stimuli, such as hormones, growth factors, and in particular, neuronal activity (Calabrese, 2006; Knott and Holtmaat, 2008; Yoshihara et al., 2009; Bosch and Hayashi, 2012; Wyatt et al., 2012). For most CNS neurons, spines contain the postsynaptic elements of excitatory synapses, and changes in spine morphology correlate with their maturation, and with alterations in synaptic efficacy (Matsuzaki et al., 2004; Tada and Sheng, 2006; Yoshihara et al., 2009; Bosch and Hayashi, 2012). Such changes modify and refine synaptic connectivity, and a variety of identified molecular signals have been shown to control these processes. Extensive evidence has demonstrated that brain-derived neurotrophic factor (BDNF) signaling, through its receptor TrkB, regulates spine formation, maturation, pruning, maintenance, and activity-dependent structural and functional plasticity (Luikart and Parada, 2006; Tanaka et al., 2008; Rauskolb et al., 2010; Kaneko et al., 2012; Vigers et al., 2012; Yoshii, 2014). The activity-dependent nature of BDNF expression and secretion makes it ideally suited to meditate the trophic effects of activity on neuronal morphology and plasticity (Gall, 1992; Shieh and Ghosh, 1999; Lessmann and Brigadski, 2009; Kuczewski et al., 2010). Much of what is known about BDNF modulation of dendritic development, spine dynamics, and synapse maturation has emerged from studies of glutamatergic cortical and hippocampal neurons, however populations of GABAergic

neurons are also morphologically responsive to this neurotrophin (Jin et al., 2003; Kohara et al., 2007; Gottmann et al., 2009; Rauskolb et al., 2010).

BDNF is normally expressed at low levels in the rodent olfactory bulb, localizing to subpopulations of neurons in the glomerular layer and outer EPL, and to scattered cells located within and near the mitral cell layer (MCL)/superficial granule cell layer (GCL), with very low expression throughout the remaining granule cell layer (Hofer et al., 1990; Guthrie and Gall, 1991; Nef et al., 2001; Conner et al., 1997; Clevenger et al., 2008). Higher olfactory regions, including some areas that provide centrifugal afferents to the bulb such as the anterior olfactory nucleus (AON) and piriform cortex, exhibit much higher levels of expression, potentially providing an anterograde source of BDNF for bulb neurons (Guthrie and Gall, 1991). TrkB is expressed by all neuronal populations in the adult olfactory bulb, whereas cellular expression of the low affinity neurotrophin receptor, p75, is limited to ensheathing glia in the olfactory nerve layer (Deckner et al., 1993; Gong et al., 1994). As with other forebrain regions, BDNF expression in the bulb is activity-responsive, with seizure activity upregulating BDNF levels and sensory deprivation reducing them (Katoh-Semba et al., 1999; McLean et al., 2001). BDNF is not required for embryonic bulb development as knockout mice show normal bulb anatomical organization during early neonatal life (Nef et al., 2001). However in those knockout mice that survive out to ~4 weeks, the olfactory bulbs are smaller and parvalbumin (PV)-expressing GABAergic neurons show impaired dendritic development and reductions in PV expression, deficits that can be rescued in vitro by BDNF administration (Berghuis et al., 2006). In vitro, differentiating GCs derived from neonatal subventricular zone (SVZ) progenitors develop more complex dendrites when treated with BDNF (Gascon et al., 2005). Its application to cultured neonatal olfactory bulb slices promotes the elaboration and branching of MTC dendrites, and increases the density of filopodia-type spines on these developing neurites (Imamura and Greer, 2009). Within such treated slices, GCs do not show alterations in spine density, however a shift in spine morphology toward thinner, longer, more filopodia-like spines is observed (Matsutani and Yamamoto, 2004). Whether augmenting BDNF levels alters the dendritic morphology of adult bulb neurons in vivo has not been determined. In the present study, we examined the effects of sustained increases in endogenous BDNF on the dendritic morphology of adult olfactory bulb GCs in vivo. Enhanced expression of BDNF by GCs in transgenic mice did not alter overall dendritic lengths or numbers of branch points in comparison to GCs in wild-type (WT) controls. However, spine numbers and densities were increased in the apical dendritic domain. These changes included a significant increase in the prevalence of mature, mushroom-like spines. Our findings suggest that increased BDNF availability can shape GC functional connectivity in the olfactory bulb by promoting dendritic spine formation and/or maintenance.

Materials and methods

Animals

All animal procedures were carried out according to protocols approved by the Florida Atlantic University Institutional Animal Care and Use Committee, in accordance with National Institutes of Health guidelines. TgBDNF mice, maintained on a C57Bl6/J

background, were obtained from Jackson Laboratories (strain #006579; Bar Harbor, ME). This strain carries a transgene encoding rat BDNF under control of 8.5 kb of the α-calcium/calmodulin-dependent protein kinase II (CAMKIIα) promoter, in addition to the endogenous BDNF gene (Huang et al., 1999). Postnatal expression of the BDNF transgene follows the developmental pattern of forebrain CAMKIIα expression, beginning near the end of first postnatal week and reaching adult levels by ~1 month of age (Neve and Bear, 1989; Zou et al., 2002). TgBDNF males were mated with WT females to obtain litters composed of transgenic and WT offspring. Genotyping was carried out by PCR amplification of genomic DNA isolated from tail samples using the following the primers for detection of the transgene: 5′-CAAATGTTGCTTGTCTGGTG-3′ and 5′-GTCAGTCGAGTGCACAGTTT-3′. Cycling parameters were as follows: 94°C-30 sec, 55°C-30 sec, 72°C-45 sec (30 cycles). To test for possible progressive effects of cell exposure to increased BDNF over time, brains were collected from young adult mice at 2–3 months of age, and from older mice aged 6–7.5 months.

In situ hybridization and densitometry

Young adult males of both genotypes (n=4 each) were euthanized with sodium pentobarbital (150 mg/kg; i.p.) at 2–3 months of age. Following decapitation, brains were rapidly dissected, snap frozen in chilled isopentane (−50°C), and stored at −80°C prior to cryosectioning. Serial sections through the bulbs and forebrain (25μm; 1 in 4) were collected on charged glass slides and were hybridized with ^{35}S-labeled BDNF cRNA as described (Guthrie and Gall, 2003). Alternate sections were stained with neutral red. The 540-base BDNF cRNA contains 384 bases complementary to the coding region of mature BDNF (GenBank sequence NM_012513). Non-specific labeling was assessed using sense RNA generated from the same template. Hybridization was conducted overnight at 65°C with the cRNA at a final concentration of 1×10^7 cpm/ml. Washing was followed by RNase A treatment to remove unbound cRNA. Sections were slide mounted and exposed to Kodak Biomax MR film (3–4 days), with tissue from paired WT and TgBDNF mice exposed on the same sheets. Densitometry was performed with NIH Image 6.2 analysis software (Wayne Rasband, NIH), with slide-mounted radiolabeled autoradiography standards used to calibrate film density (American Radiolabeled Corp., St. Louis, MO). Multiple measures were collected by overlay of adjacent sample boxes positioned around the full circumference of the granule cell layer (GCL) from a minimum of 8 sections per animal (both bulbs), with background density measured in the olfactory nerve layer subtracted from these measures for each section. Section means were used to calculate mean GCL labeling density (dpm/mg protein) for each animal. Group mean values +/− standard error of the mean (SEM) were calculated from these values, and effect of genotype was assessed using unpaired t-test comparisons, with significance defined as $p<0.05$. No specific labeling patterns were observed in sections incubated with radiolabeled sense RNA. Following film exposure, sections were processed for emulsion autoradiography using Kodak NTB and exposure times of 5–6 weeks. After development, sections were counterstained with neutral red, and microscope images of cell labeling were collected with an Olympus AX70 microscope equipped with a Magnafire digital camera. All figures were assembled using Adobe Photoshop CS3, with adjustments made for size, orientation, contrast and brightness.

BDNF Enzyme-Linked Immunosorbent Assay (ELISA)

Mice at 2–3 months of age (4 per genotype; 2 male, 2 female) were euthanized as above, decapitated, and the olfactory bulbs rapidly dissected. Tissue was frozen on dry ice and stored at −80°C. Both olfactory bulbs were homogenized together on ice in Cell Lysis buffer (#9803, Cell Signaling Technology, Danvers, MA) to which 1mg/ml complete protease inhibitors and 1 mg/ml complete phosphatase inhibitors (Roche Applied Biosystems) were added. Lysates were centrifuged at 14,000 rpm for 20 min at 4°C and supernatants were collected and assayed for protein content by Qubit assay (Invitrogen, Carlsbad, CA). Aliquots were stored at −80°C, prior to performing ELISA assays or Western blotting. ELISA plates were treated overnight with monoclonal antibody to BDNF, according to the manufacturer's instructions for the BDNF Emax immunoassay system (Promega, Madison, WI, USA). Supernatants were thawed and diluted 1:3 in Dulbecco's phosphate-buffered saline. Samples were acidified by adding 2 μl of 1N HCl per 100μl solution, and were incubated for 20 min at room temperature (RT). The pH was normalized by then adding 2μl of 1N NaOH per 100μl of sample. Duplicate samples (150 μg protein/well) incubated overnight at 4°C, and were assayed for total BDNF protein content (pro- and mature BDNF), according to the Emax kit instructions. A standard curve was generated for each assay using serial dilutions of recombinant BDNF peptide provided in the kit. Following color development, absorbance was measured at 450nm using a SpectraMax M5 plate reader (Molecular Devices, Sunnyvale, CA), and BDNF concentrations in samples were calculated using SoftMax Pro software. T-test comparisons of group mean values (+/− SEM) were used to determine significance of genotype ($p<0.05$).

Western blotting

Olfactory bulb lysates prepared from tissue samples (as above) were thawed, diluted in Laemmli buffer and denatured at 95°C for 5 min. Protein was separated by 12% SDS-PAGE (BioRad TGX gels). Control lanes for BDNF blots included 5 ng of human recombinant mature BDNF peptide (PeproTech, Rocky Hill, NJ). Proteins were transferred to PVDF membranes (0.45μm) and blocked Odyssey blocking buffer (Li-Cor Biosciences, Lincoln, NE) for 1 hr at RT. Purified polyclonal rabbit IgG antibody to BDNF was from Santa Cruz Biotech (Santa Cruz, CA; Cat# sc-546.) It was generated using mature, human BDNF as antigen (amino acid residues 128-147: RHSDPARRGELSVCDSISEW; manufacturer's data), and does not cross-react with other members of the neurotrophin family. It detects mature BDNF at ~14 kDa on immunoblots of hippocampal lysates from normal mice, while this band is absent on blots of hippocampal lysates prepared from BDNF knockout mice (Matsumoto et al., 2008). Mouse monoclonal anti-actin antibody was obtained from Cell Signaling Technologies (Danvers, MA, #3700). It was generated against a synthetic peptide corresponding to amino-terminal residues of human β-actin, and detects a single band of ~42–43 kDa molecular mass in immunoblots of COS and HeLa cells (manufacturer's data). BDNF antibody (1:200) and actin antibody (1:1000) were diluted together in Odyssey blocker, with 0.2% Tween 20 added. Membrane incubation was carried out at 4°C for 2 nights. After rinsing in Tris-buffered saline (TBS; 50 mM Tris-HCl, 150 mM NaCl, pH 8.2), containing 0.1% Tween-20 (TBST), membranes incubated in a cocktail of Dylight infared dye-labeled IgGs (Thermo Scientific) specific for rabbit (dye 680) and mouse (dye 800), both diluted 1:5000 in TBST, for 1 hr. Blot images were examined and digitized using the

Li-Cor Odyssey Fc imaging system. For semi-quantitative comparisons, band intensities were normalized to actin bands in the same lane, and quantified using Li-Cor Odyssey software. Levels of protein measured from blot samples obtained from transgenic mice (n=4) are expressed as the mean fold-difference (% of control) in normalized band intensities relative to measures from WT samples (n=4) on the same blot.

Golgi-Cox staining

Adult mice of both sexes were euthanized as above at 2–3 months of age, or at 6–7.5 months of age. Mice were then perfused transcardially with ice-cold phosphate-buffered saline (PBS, pH 7.3, 200 mls). Brains were dissected and processed using a modified Golgi staining technique as described (Isgor and Sengelaub, 2003). At 2–3 months of age, brains from 2 WT mice (1 male, 1 female) and 3 TgBDNF mice (2 male, 1 female) were processed for impregnation. At 6–7.5 months of age, brains from 3 WT (1 male, 2 female) and 3 TgBDNF mice (1 male, 2 female) were processed. Brain tissue was submerged in Golgi-Cox solution containing 5% potassium dichromate, 5% mercuric chloride, and 5% potassium chromate in distilled water, and were stored in the dark for 30 days. The solution was replaced every 2–3 days. Brains were then dehydrated and embedded in celloidin. Coronal microtome sections through both olfactory bulbs (160μm) were cut and processed according to the protocol described by (Glaser and Van der Loos, 1981), without counterstaining. Treatment included alkalinization in ammonium hydroxide (66%), development in Kodak Dektol and fixation in Kodak photographic fixative. Sections were dehydrated through increasing concentrations of ethanol, and cleared in xylene before mounting. To accommodate tissue thickness, sections were mounted on custom-made made glass slide compartments using Permount, and were air-dried for several weeks before analyses.

Analyses of dendritic morphology

Olfactory bulb granule cells were reconstructed at 100X objective magnification using a motorized Axiophot 2-Plus microscope (Zeiss, Germany) equipped with a Microfire digital camera (Optronics, CA). Examples of Golgi-impregnated cells are shown in Figures 1A–B. For mice at 2–3 months of age, a total of 42 cells from WT mice and 47 cells from TgBDNF mice were reconstructed (minimum of 9 cells per animal). To test the effects of longer exposure to increased BDNF with age, granule cells from 6–7.5 month-old mice were also reconstructed (42 cells for WT, 47 cells for TgBDNF, minimum of 12 cells per animal). Three-dimensional, computer-based neuronal tracing and reconstruction, as well as data collection and analyses, were performed using NeuroLucida and NeuroExplorer software (MicroBrightfield, Inc., Williston, VT). Selection criteria for reconstruction and analysis of individual granule cells included the following: 1) full impregnation of the cell to ensure visibility of the soma, dendrites and spines, with dendrites remaining intact within the section thickness, 2) no obstruction of the dendrites or soma by other stained cells or artefacts, 3) apical dendrites extending past the mitral cell layer and 4) morphology characteristic of mature granule cells, including the presence of dendritic spines, and an apical dendrite with at least one branch point (Carleton et al., 2003). Cells with immature features (emerging from the subpendymal layer, dendritic beading, absence of spines, no apical branching) were excluded. Those with few or no visible basal dendrites were included if the apical dendrite and soma were well impregnated and bore spines. While

reconstructions were limited to cells with mature features, turnover of the mouse GC population leads to continuous, gradual GC cell replacement throughout life (Imayoshi et al., 2009). New cells are generated from progenitors in the adult forebrain SVZ, and from here, thousands of immature GCs migrate into the bulb daily (Alvarez-Buylla and García-Verdugo, 2002). About half of these undergo apoptosis during migration and early development, but those that survive undergo maturation and functional integration over a period of ~8 weeks, with dendrites achieving adult-like morphology when cells are ~1 month old (Carleton et al., 2003; Mizrahi, 2007; Whitman and Greer, 2007; Kelsch et al., 2009; Pallotto et al., 2012). Therefore populations of reconstructed cells from individual mice are likely to have included GCs of different cell age.

Measurements of dendritic morphology included total, apical and basal dendritic lengths, numbers of dendritic branch points (bifurcations/nodes), and number of terminal branches per cell. Sholl analysis of apical dendrite complexity was performed by counting the number of dendritic segments intersecting concentric spheres (20μm intervals) superimposed on reconstructed cells, with the cell soma at the center. Cell soma distance from the MCL/EPL border also was measured. Because a subset of reconstructed cells in all mice lacked visible basal dendrites, data collected for basal measurements at 2–3 months were obtained from 34 cells in WT mice, and 37 cells from TgBDNF mice. At 6–7.5 months, 36 and 32 cells, from WT and TgBDNF mice, respectively, were used. For those cells lacking basal dendrites, values calculated for total dendritic measurements (total length, total spine number) were the equivalent of values obtained for the apical compartment alone.

Analyses of dendritic spines

Spines were inspected on both apical and basal dendrites of olfactory bulb granule cells, and as illustrated in figure 1C, were classified into 3 categories (adapted from Hering and Sheng (2001) and Naritsuka et al., 2009): 1) Headed spines, considered mature or stable (Knott et al., 2006), included all spines with a neck (regardless of neck length) supporting a bulbous spine head that exceeded the width of the neck, 2) elongated, filopodia-like spines, considered immature (Holtmaat et al., 2005), were defined as long spines (>2.5μm) lacking enlargement of the tip, and 3) other-type spines that did not fall into the either of the above categories. The latter group consisted primarily of short, headless spines extending <2.5μm from the shaft (regardless of thickness, dotted arrow in Fig. 1C), and other, stubby spines that appeared as raised bumps on the shaft with no neck. Spines in the other-type category may be spines in morphological transition from other spine types, particularly filopodia, which exhibit rapid formation and retraction on the dendrites of adult-born GCs (Parnass et al., 2000; Breton-Provencher et al., 2014). Spines on the soma were not included in analyses due to the difficulty in resolving them against the dense staining of the cell body. Dendritic spine analyses included calculation of total number and density per cell, spine number and density in apical and basal dendritic compartments, number and density of individual spine types, and proportions of spines in each category. In order to assess if differences in spine density varied with distance along apical dendrites, NeuroExplorer software was used to calculate density in three domains along apical dendrites: the most proximal domain (within 50μm of the soma), the middle domain (the next 50μm), and the outer apical dendrite (remaining dendrite beyond the first 100μm).

Comparisons of group mean measures obtained from WT and TgBDNF mice at 2–3 months were performed using unpaired, two-tailed t-tests, with significance defined as $p<0.05$. Group mean values per genotype were also compared by unpaired, two-tailed t-tests for the 6–7.5 month-old animals. Age effects were tested using unpaired t-tests to compare group means obtained from WT mice at 2–3 months and 6–7.5 months, and means obtained from TgBDNF mice at 2–3 months versus 6–7.5 months, with significance define as $p<0.05$. Unless otherwise stated, results are reported as group mean values +/− the standard error of the mean (SEM). Additionally, to test for significant interaction, two-way ANOVA was performed for all measures, with Genotype and Age as between-subjects variables.

Results

BDNF mRNA and protein levels are increased in the transgenic olfactory bulb

While in most areas of forebrain, CAMKIIα is expressed by glutamatergic projection neurons, in the olfactory bulb it is expressed by GABAergic granule cells and a subpopulation of glomerular neurons; it is not expressed by mitral or tufted cells (Benson et al., 1992; Zou et al., 2002; Néant-Fery et al., 2012). Therefore, BDNF expression under control of the CAMKIIα promoter would drive BDNF transgene expression in the GC population as it develops postnatally, with ongoing GC expression in the adult bulb. Mitral cells would lack transgene expression. We confirmed this in young adult mice using in situ hybridization of ^{35}S-labeled BDNF riboprobe. Bulb sections stained with neutral red showed normal laminar organization of olfactory bulb cell populations (Fig. 2A). Alternate sections processed for BDNF cRNA labeling showed patterns of hybridization consistent with the reported distribution of normal BDNF mRNA expression in control, WT mice, and with the known distribution of bulbar CAMKIIα expression (Fig. 2B). Adult TgBDNF mice expressed significantly higher levels of BDNF mRNA in the GCL compared to their WT counterparts (Figs. 2B–D). Additional cRNA labeling of cells distributed in the glomerular region occurred in all mice, with enhanced silver grain density overlying some of these cells in TgBDNF mice (Figs. 2E–F). On film autoradiograms, the labeling of scattered cells within the superficial GCL-MCL region was suggestive of MCL labeling, however when examined microscopically for silver grain accumulation, neutral-red stained mitral cells were not labeled by the ^{35}S-tagged BDNF cRNA in either WT or TgBDNF mice, similar to results reported by Clevenger et al. (2008), and consistent with the documented lack of CAMKIIα expression by mitral cells (Zhou et al., 2002; Néant-Fery et al., 2012) (Figs. 2E–F). The identity of the scattered, well-labeled cells in the MCL-superficial GCL region could not be determined in our emulsion-processed tissue sections. Their location in both WT and TgBDNF mice is consistent with the distribution of multiple classes of cells, including types of short axon cells, superficial granule cells, and mitral/deep tufted cells. That only a few, scattered cells were labeled in this region may be cell-type specific, but as normal BDNF gene expression is activity-dependent, it may reflect increased levels of recent physiological activity within individual short axon, granule, or mitral/tufted cells. Alternatively, the chromosomal location of the (CAMKIIα) - BDNF transgene insertion may have an unanticipated influence on BDNF expression in one or more of these cell types in TgBDNF mice, raising the possibility that some of the labeled cells in the MCL shown in figure 2F are mitral/tufted cells. Piriform cortex and the AON, both areas that provide centrifugal

innervation of GCs, also showed increased BDNF mRNA expression in TgBDNF mice relative to WT controls (Fig. 2C). BDNF mRNA increases were accompanied by increased BDNF protein levels measured by ELISA. Olfactory bulb BDNF protein content (total) measured significantly higher in transgenic mice, in comparison to the very low levels detected in WT littermates (Fig. 3A). Increases in mature BDNF protein contributed to this change. Immunoblots of bulb lysates showed bands corresponding to mBDNF at ~14kDa, with those from transgenic mouse samples showing increased band intensity relative to WT samples (Figs. 3B–C).

Granule cell dendritic lengths and branch complexity

Morphometric analyses were performed to test for BDNF effects on GC dendritic complexity. Examples of reconstructed cells are illustrated in figure 4. The morphology of the GC population in the adult rodent bulb is heterogeneous, with multiple subtypes of GCs recognized based on location of the soma, dendrite distributions, and dendrodendritic synaptic partners (mitral vs tufted cells) (Nagayama et al., 2014). Based on the distribution of apical dendrites, the majority of our reconstructed cells were of type 1 or 2 as described by Greer (1987), as well as a small number of superficial GCs that were similar to type V cells (shrub-type, Nagayama et al., 2014). As illustrated in figures 5A–B, unpaired t-test comparisons of measures from TgBDNF mice and age-matched WT controls showed no significant differences in mean apical, basal or total dendritic lengths ($p>0.05$). However older TgBDNF mice had shorter mean apical dendritic lengths compared to 2–3 month-old TgBDNF mice (Figs. 5A–B; $p<0.05$, unpaired t-test). Mean numbers of total and apical dendritic branch points did not differ between age-matched WT and TgBDNF mice at any age. Apical dendrite branch points ranged in number from 1–7 per cell in individual mice. At 2–3 months, sampled cells in WT mice averaged 2.41 +/−0.09 (SEM) branch points, and TgBDNF mice averaged 2.74 +/−0.14 ($p>0.05$, unpaired, two-tailed t-test). Apical terminal branch endings ranged from 2–8 per cell and mean values did not differ with genotype at either age (2–3 months, WT= 3.43 +/−0.7, Tg= 3.76 +/−0.15, $p>0.05$, unpaired t-tests). Sholl plots of apical dendritic intersections showed no significant effects of genotype at either age ($p>0.05$ for all intersection/distance points, t-tests, Figs. 5C–D).

Two-way ANOVA indicated no interaction of Age and Genotype for any morphometric measures made in this study, with the exception of apical dendritic length ($F_{1,10}=10.79$, $p=0.013$).

Over-expression of BDNF by GCs increases their dendritic spine number and density

We next focused our analyses on changes in dendritic spines, and in particular, mature headed types. Figures 6A–D illustrate the effects of increased GC expression of BDNF on numbers of GC dendritic spines. In young adults, mean total spine number in WT mice measured 79.8 +/−5.4 (SEM), compared to 130.8 +/−11.5 in transgenic mice ($p<0.05$, unpaired, two-tailed t-test, $t_{(3)}=3.31$). Mean spine numbers in the older animals measured 80.9 +/−8.9 for WT mice and 119.0 +/−2.0 in TgBDNF mice ($p<0.05$, unpaired t-test, $t_{(4)}=4.18$). Changes in total numbers included increases in numbers of headed spines in TgBDNF mice at both ages. Headed spines, which included gemmules, were the most prevalent type observed, and at 2–3 months, TgBDNF mice averaged ~25% more, (WT=

49.8 +/−0.9, Tg= 69.2 +/−1.9, $p<0.01$, unpaired t-test, $t_{(3)}=7.76$), a difference that remained stable when compared to mean numbers in older mice (WT= 46.8 +/−4.1, Tg= 67.4 +/−1.9, $p<0.01$, t-test, $t_{(4)}=4.56$). As apical dendrites make the largest contribution to total measures, results for the apical compartment alone were similar (at 2–3 months, WT= 42.5 +/−1.7 headed spines, Tg= 62.6 +/−0.8, $p<0.01$, unpaired t-test, $t_{(3)}=12.14$). Numbers of other-type spines in apical dendrites were not significantly different at either age.

In basal dendrites, group mean values for total spine numbers did not differ significantly, though they trended higher in older transgenic mice (20.2 +/− 3.4 versus 10.4 +/− 3.5 in age-matched controls, $p=0.11$, unpaired t-test). Long filopodia-like spines (>2.5 um) were the least abundant type, and varied widely in number across cells in all animals (2–20 per cell). They were found in all portions of apical dendrites and in basal dendrites. Mean numbers of filopodia per cell did not differ with genotype at any age (at 2–3 months, WT= 3.00 +/−0.44, Tg= 7.43 +/−1.60, $p=0.11$, unpaired t-test). The relative proportions of different spine types comprising the total spine numbers for each group are illustrated in figure 7. For all measures of spine numbers, there were no significant age-associated differences within either the WT or transgenic groups.

As shown in figures 8A–D, total spine density differed with genotype, as did the density of headed, mature spines (Figs. 8A–D). At 2–3 months, total spine density per cell measured 0.31 +/−0.02 per μm in WT mice, and 0.47 +/− 0.02 per μm in TgBDNF mice ($p<0.05$, t-test, $t_{(3)}=4.47$), values that remained stable with age. Within apical dendrites, headed spine density in young adult TgBDNF mice (0.237 +/−0.006 per μm) exceeded that of WT mice (0.185 +/−0.005 per μm) by ~20% ($p<0.05$, t-test, $t_{(3)}=5.51$), a difference that reached ~30% in older animals ($p<0.05$, unpaired t-test). No significant effects of age on total or apical spine density, or mature spine density, were measured within either genotype ($p>0.05$, unpaired t-tests). Basal dendritic spine density was higher in young adult TgBDNF mice compared to WT controls ($p<0.05$, t-test), possibly due to changes in distribution as spine numbers did not differ significantly, however differences in older mice did not reach significance.

BDNF-mediated changes in spine density occur in proximal and distal dendritic domains

Within proximal apical dendritic segments, genotype affected spine density in both age groups. As illustrated in figures 8E–F, young adult TgBDNF mice had higher mean densities here (0.47 +/−0.04 spines/μm), while values from WT mice were significantly lower (0.31 +/−0.01 spines/μm, $p<0.05$, unpaired t-test, $t_{(3)}=3.35$). The middle domain, which for most cells contained that portion of the dendrite that traversed the MCL, did not display significant differences in spine density with genotype ($p>0.05$, t-tests). However the most distal apical compartment exhibited greater mean spine density in TgBDNF mice at both ages, compared to age-matched controls (at 2–3 months, TgBDNF = 0.46 spines/μm +/−0.03, WT = 0.31 spines/μm +/−0.01, $p<0.05$, t-test, $t_{(3)}=3.79$).

Discussion

Normal processing of odor information in the olfactory bulb relies on the functional connectivity of the inhibitory GC population. Their dendritic morphology establishes the

framework for this connectivity, and here we used Golgi-Cox impregnation, 3D reconstruction and morphometric analyses to show that sustained elevations in endogenous BDNF modify this morphology by increasing the number and density of spines in vivo. This includes an increased prevalence of mature spines in the apical compartment where reciprocal GC-MTC synapses are located. The increase in spine density is present in TgBDNF mice by 2–3 months, and quantitative comparisons with older mice indicate that it persists with age. Our findings demonstrate that changes in BDNF availability in vivo can shape structural features of GC dendritic connectivity within adult olfactory circuitry. These results complement recent findings by Bergami et al. (2013) showing reduced spine density in adult-born GCs in which BDNF signaling is eliminated by TrkB deletion.

Apical dendrite spine numbers and densities in our control mice are similar to those reported by Charles Greer (1987) in a Golgi study of heterozygous control mice of the mutant Purkinje Cell Degeneration strain. We obtained spine densities averaged over the full length of the apical dendrite that ranged from ~0.27–0.30 spines/μm, results that also compare favorably with densities obtained from adult-born GCs labeled by gene transfer of green fluorescent protein (GFP) (Dahlen et al., 2011). The density of mushroom spines on distal apical dendrites has been measured at ~0.20/μm in mature GCs imaged in acute bulb slices and our results, averaged over the full apical dendrite of WT mice (~0.18/μm), are again in good agreement (Breton-Provencher et al., 2014). Of note in our Golgi material is the scarcity of filopodia-type spines on our sampled cells compared to numbers reported for adult-born cells expressing GFP, which we attribute to our criterion of filopodia as long, headless extensions of 2.5μm or more (Whitman and Greer, 2007; Breton-Provencher et al., 2014). Shorter, thin spines as well as short, thicker spines and stubby profiles were classified as other-types, and process diameter was not measured to further subdivide spine types. By this classification, short filopodia would have been included in this category. As described for other neurons, spines in the other-type category are likely to include non-stabilized spines undergoing morphological transitions, an indication of ongoing spine plasticity within the GC population (Parnass et al., 2000; Holtmaat et al., 2005). In vivo imaging of adult-born GCs has shown rapidly dynamic changes in spines even in mature cells, and in as little as 20 min, the full cycle of spine emergence from an initial stubby protuberance, extension into a filopodium, retraction and final disappearance can be observed (Mizrahi, 2007; Breton-Provencher et al., 2014). The proportion of spines that fell into the other-type category, by our criteria, remained relatively stable at ~35% of the total numbers per cell across mice of both ages and genotypes. If many of these are in fact spines in transition, this would indicate that GCs maintain a fairly high level of spine plasticity even when mature, as has been elegantly shown by in vivo imaging of adult-born cells (Mizrahi, 2007).

The increase in headed spines seen with GC over-expression of BDNF in vivo contrasts with some actions observed in cultured neonatal bulb slices, in which the predominant effect of exogenous BDNF administration was an increase in filopodia-type spines on developing GCs, as well as enhanced dendritic branching (Matsutani and Yamamoto, 2004). Differences in cell maturational state, the manner in which the cells are exposed, as well as patterns of neural activity in vitro versus in vivo may contribute to this, as suggested by the variability of BDNF effects on hippocampal neurons. In vivo, BDNF over-expression in the adult TgBDNF hippocampus increases spine density on CA1 pyramidal cells, while

conditional ablation of BDNF promotes a shift to longer, thinner spines, with no change in density (An et al., 2008; Rauskolb et al., 2010). Blocking endogenous BDNF in vitro similarly increases the prevalence of longer, thinner, immature spines in pyramidal cells, but also reduces spine density (Kellner et al., 2014). Treatment with exogenous BDNF has little effect on dendritic morphology of mature pyramidal cells, but immature cells respond with enhanced dendritic branching (Kellner et al., 2014). Spine density in mature cells can be decreased by suppressing activity in vitro, and TrkB-IgG treatment reduces density further. Exogenous BDNF can reverse the latter effect, but not the effect of activity blockade, evidence that even in vitro, BDNF actions on spine maintenance depend on activity levels (Kellner et al., 2014).

While Golgi-Cox staining does not demonstrate the presence of synapses, the greater numbers and densities of headed spines on GC apical dendrites in TgBDNF mice suggests that BDNF can promote the formation and/or maintenance of glutamatergic synapses in this domain, particularly reciprocal synapses with MTCs. Differences in spine density on proximal and basal dendrites also occurred, potentially reflecting effects on other innervating populations. GC activity is regulated by multiple excitatory inputs that are spatially organized along the dendritic arbor according to innervation source (Shepherd, 2004; Balu et al., 2007; Laaris et al., 2007; Kelsch et al., 2008). In addition to gemmule-located MTC synapses, spines located on GC basal dendrites, somata and proximal apical dendrites receive axodendritic and axosomatic synapses from excitatory centrifugal afferents originating from the AON and piriform cortex (Shepherd, 2004; Matsutani and Yamamoto, 2008; Deshpande et al., 2013). Axon collaterals from MTCs are thought to innervate the deeper dendritic domains of GCs as well (Kishi et al., 1984). Small numbers of GABAergic synapses have been localized to GC spines also, though most terminate on dendritic shafts. These arise from local GABAergic short axon cells, and centrifugal projections from the horizontal limb of the diagonal band of Broca (Eyre et al., 2008; Gracia-Llanes et al., 2010; Arenkiel et al., 2011; Deshpande et al., 2013).

The GC population is initially generated during the first three postnatal weeks in rodents, following the embryonic development of MTCs (Brunjes and Frazier, 1986). During postnatal development, and thereafter as continuing neurogenic activity in the SVZ produces new cells, developing and mature GCs in TgBDNF mice are exposed to levels of endogenous BDNF that are significantly higher than normal, as shown by our ELISA results. Whether born during the early postnatal period or in adulthood, GCs arriving in the bulb express full-length TrkB receptors as they mature, thereby becoming BDNF-responsive (Nef et al., 2001; Bergami et al., 2013). In TgBDNF mice, increases in GC-expressed BDNF, through dendritic and somatic release, may then act as an autocrine or paracrine factor on the GCs themselves. In vivo, genetic manipulation of BDNF expression in individual cortical and hippocampal neurons promotes enhanced spine development and maintenance in those neurons with higher expression levels, relative to neighboring cells with less, suggesting autonomous actions (English et al., 2012; Wang et al., 2015). As shown by Horch and Katz (2002), paracrine BDNF effects on neighboring cells, as well as autocrine effects, occur in neonatal cortical slices, where release of BDNF from over-expressing pyramidal cells acts over short distances (~4.5μm) to increase dendritic

branching of neighboring neurons, an effect blocked by inhibiting BDNF signaling with TrkB-IgG treatment.

As also shown in developing cortical slices, BDNF can act as a classic, target-derived signal, promoting the development and maturation of presynaptic inputs. Single cell gene knockout of BDNF in pyramidal cells reduces numbers of GABAergic terminals that form on somata of BDNF-depleted cells compared to those with normal expression (Kohara et al., 2007). Conversely, in the TgBDNF mouse strain, functional maturation of inhibitory circuitry in visual cortex is accelerated by BDNF over-expression in vivo, reducing the duration of the sensory critical period, and consistent with its ability to increase $GABA_A$ receptor expression in cultured visual cortical neurons (Huang et al., 1999; Mizoguchi et al., 2003). Increased spine density in GC apical, proximal, and basal dendrites raises the possibility that in TgBDNF mice, excess BDNF may modify inputs from multiple TrkB-expressing neuronal populations that terminate on different portions of the dendritic tree. Spine plasticity within the proximal dendrite, targeted by excitatory afferents from olfactory cortex, occurs with olfactory learning, producing increased spine density in this domain and in basal dendrites on adult-born GCs (Lepousez et al., 2014). GC over-expression of BDNF may alter spine density in these compartments by remodeling cortical input, although piriform cortex itself expresses BDNF in both normal and TgBDNF mice, with potential anterograde effects on spine plasticity. GABAergic terminals may be altered as well, and this inhibitory input has been shown to be crucial to the functional integration of adult-born GCs, and to their dendritic development in particular (Pallotto et al., 2012). As noted above, BDNF has demonstrated actions on development of CNS GABAergic circuitry in TgBDNF mice. Further work is needed to evaluate changes in the expression and/or distribution of pre- and postsynaptic specializations on GC dendrites to determine if increased BDNF alters excitatory or inhibitory connectivity, and what the potential functional implications of such changes might be.

MTCs express TrkB, and there is evidence to suggest that these output neurons initiate the formation of dendrodendritic synapses (Hinds and Hinds, 1976; Panzanelli et al., 2009). As these synapses are formed and later maintained, the excess BDNF produced by GCs in transgenic mice may act on the output neurons via this route. While for other neurons dendritic secretion constitutes post-synaptic release, GCs are unique in that within dendrodendritic synapses, they are structurally and functionally both pre- and postsynaptic to MTCs. Evidence for dendritic secretion of BDNF is based on in vitro studies of hippocampal and cortical neurons, but remains to be unequivocally demonstrated in the brain. Neurons expressing GFP- or pHluorin-tagged BDNF traffic the protein through the constitutive and regulated secretory pathways, and transport BDNF via dense core vesicles in axons and in dendrites, for release from both, though this may not apply to all types of neurons (Gottmann et al., 2009; Kuczewski et al., 2010; Edelmann et al., 2014). BDNF is differentially trafficked in dendrites and axons, and BDNF-containing vesicles can be recruited in a stimulation-dependent fashion to activated synaptic sites in both dendrites (postsynaptic) and axons (presynaptic) (Dean et al., 2012). Moreover, BDNF can be released from dendrites, in a Ca+2-dependent manner, in response to prolonged depolarization or theta burst stimulation (Magby et al., 2006; Kolarow et al., 2007; Matsuda et al., 2009). Synthesis of BDNF protein in dendrites is further suggestive of a dendritic mode of action

for this neurotrophin. Neurons produce two mRNAs from the normal BDNF gene, one of which, containing a long 3′ untranslated region (UTR), is dendritically transported for local translation, while the short 3′ UTR mRNA remains in somata (An et al, 2008). In vitro and in vivo, somatic translation of the short 3′ UTR mRNA promotes spine formation, whereas dendritic synthesis of BDNF from the long 3′ UTR mRNA is required for normal spine maturation and age-dependent pruning (Kaneko et al., 2012; Orefice et al., 2013). Olfactory GCs, like other neurons, are capable of dendritic transport of specific, native mRNAs, and may therefore be capable of local dendritic protein translation as well (Néant-Fery et al., 2012). The BDNF transgene mRNA expressed in TgBDNF mice lacks the normal 3′ UTRs, and the expressed mRNA is not transported in dendrites (An et al., 2008). However, somatically translated BDNF protein would undergo typical vesicular packaging, and axonal and dendritic trafficking in the CNS neurons that over-express BDNF in this strain, accounting for its described effects in vivo (Huang et al., 1999; An et al., 2008; Gharami et al., 2008).

Our findings do not address whether the increase in GC spine density in TgBDNF mice reflects ongoing addition, initial over-production during cell development, or maintenance of spines that would otherwise be lost via activity-dependent adjustments at later stages. Detailed studies of adult-born cells have shown that during their early development, GCs initially overproduce apical dendritic spines as they integrate into local circuitry, then reduce spine density as they mature further, presumably via pruning mechanisms that work to fine tune functional connectivity in response to activity (Whitman and Greer, 2007; Nissant and Pallotto, 2011; Pallotto et al., 2012). Increased BDNF in the context of postnatal network activity may enhance the maturation and retention of GC spines that would otherwise be unstabilized and eliminated over time. This interpretation would be consistent with results from adult-onset, forebrain-specific BDNF knockouts that demonstrate the requirement of BDNF for long-term spine maintenance in vivo (Rauskolb et al., 2010; Kaneko et al., 2012; Vigers et al., 2012). However, as noted above, somatic synthesis of over-expressed BDNF can promote spine formation during neuronal development (An et al., 2008; Orefice et al., 2013). The increase in the density of mature, headed spines on GCs in this mouse strain is suggestive of sustained effects on spine maintenance, but examination of GCs during their early stages of development will be needed to address potential changes in the initial elaboration of dendrites and spines in response to increased BDNF.

BDNF-dependent modifications in spine numbers and morphology have been documented in a number of populations of TrkB-expressing CNS neurons, and we show here that olfactory GCs are similarly responsive to changes in endogenous BDNF levels. Activity plays a role in maintaining normal GC dendritic morphology in the adult bulb, and the activity-dependent nature of BDNF release makes this an attractive candidate factor for facilitating GC spine maturation and maintenance in response to environmental sensory cues (Kelsch et al., 2009; Dahlen et al., 2011). Recent demonstrations of GC spine remodeling with olfactory learning also suggest parallels to BDNF-mediated synaptic plasticity in this context (Tanaka et al., 2008, Vigers et al., 2012; Lepousez et al., 2014; Zagrebelsky and Korte, 2014). Taken together, the demonstrations that BDNF enrichment can increase GC spine density, while inhibition of TrkB signaling can reduce it, point to a role for

endogenous BDNF signaling in modulating GC dendritic connectivity in vivo (Bergami et al., 2013).

Acknowledgments

Supported by National Institutes of Health grant DC012425 to K.G. We thank Dr. Cigdem Aydem for assistance with Golgi-Cox staining procedures and Shamayra Smail for assistance with mouse breeding, genotyping and colony maintenance.

Abbreviations

ANOVA	analysis of variance
AOB	accessory olfactory bulb
AON	anterior olfactory nucleus
BDNF	brain-derived neurotrophic factor
CAMKIIa	alpha-calcium/calmodulin dependent kinase II
CNS	central nervous system
cRNA	complementary RNA
ELISA	Enzyme-Linked Immunosorbent Assay
EPL	external plexiform layer
GABA	gamma-aminobutyric acid
GC	granule cell
GCL	granule cell layer
GFP	green fluorescent protein
mBDNF	mature BDNF
MTC	mitral/tufted cell
MCL	mitral cell layer
mRNA	messenger RNA
NMDA	N-methyl-D-aspartate
p75	low affinity neurotrophin receptor
PBS	phosphate buffered saline
pir	piriform cortex
SDS-PAGE	sodium dodecyl sulfate-polyacrylamide gel electrophoresis
str	striatum
SVZ	subventricular zone
TBS	Tris-buffered saline
TgBDNF	transgenic CAMKIIa-BDNF mouse strain

TrkB	tropomyosin receptor kinase B
UTR	untranslated region
WT	wild-type

References

Abraham NM, Egger V, Shimshek DR, Renden R, Fukunaga I, Sprengel R, Seeburg PH, Klugmann M, Margrie TW, Schaefer AT, et al. Synaptic inhibition in the olfactory bulb accelerates odor discrimination in mice. Neuron. 2010; 65:399–411. [PubMed: 20159452]

Alvarez-Buylla A, García-Verdugo JM. Neurogenesis in adult subventricular zone. J Neurosci. 2002; 22:629–634. [PubMed: 11826091]

An JJ, Gharami K, Liao G-Y, Woo NH, Lau AG, Vanevski F, Torre ER, Jones KR, Feng Y, Lu B, et al. Distinct role of long 3′ UTR BDNF mRNA in spine morphology and synaptic plasticity in hippocampal neurons. Cell. 2008; 134:175–187. [PubMed: 18614020]

Arenkiel BR, Hasegawa H, Yi JJ, Larsen RS, Wallace ML, Philpot BD, Wang F, Ehlers MD. Activity-induced remodeling of olfactory bulb microcircuits revealed by monosynaptic tracing. PLoS ONE. 2011; 6:e29423.10.1371/journal.pone.0029423 [PubMed: 22216277]

Balu R, Pressler RT, Strowbridge BW. Multiple modes of synaptic excitation of olfactory bulb granule cells. J Neurosci. 2007; 27:5621–5632. [PubMed: 17522307]

Benson DL, Isackson PJ, Gall CM, Jones EG. Contrasting patterns in the localization of glutamic acid decarboxylase and Ca2+/calmodulin protein kinase gene expression in the rat central nervous system. Neuroscience. 1992; 46:825–849. [PubMed: 1311814]

Bergami M, Vignoli B, Motori E, Pifferi S, Zuccaro E, Menini A, Canossa M. TrkB signaling directs the incorporation of newly generated periglomerular cells in the adult olfactory bulb. J Neurosci. 2013; 33:11464–11478. [PubMed: 23843518]

Berghuis P, Agerman K, Dobszay MB, Minichiello L, Harkany T, Ernfors P. Brain-derived neurotrophic factor selectively regulates dendritogenesis of parvalbumin-containing interneurons in the main olfactory bulb through the PLCγ pathway. J Neurobiol. 2006; 66:1437–1451. [PubMed: 17013928]

Bosch M, Hayashi Y. Structural plasticity of dendritic spines. Curr Opinion Neurobiol. 2012; 22:383–388.

Breton-Provencher V, Cote D, Saghatelyan A. Activity of the principal cells of the olfactory bulb promotes a structural dynamic on the distal dendrites of immature adult-born granule cells via activation of NMDA receptors. J Neurosci. 2014; 34:1748–1759. [PubMed: 24478357]

Brunjes PC, Frazier LL. Maturation and plasticity in the olfactory system of vertebrates. Brain Res. 1986; 396:1–45. [PubMed: 3518870]

Bywalez WG, Patirniche D, Rupprecht V, Stemmler M, Herz AVM, Pálfi D, Rózsa B, Egger V. Local postsynaptic voltage-gated sodium channel activation in dendritic spines of olfactory bulb granule cells. Neuron. 2015; 85:590–601. [PubMed: 25619656]

Calabrese B. Development and regulation of dendritic spine synapses. Physiology. 2006; 21:38–47. [PubMed: 16443821]

Carleton A, Petreanu LT, Lansford R, Alvarez-Buylla A, Lledo P-M. Becoming a new neuron in the adult olfactory bulb. Nat Neurosci. 2003; 6:507–518. [PubMed: 12704391]

Chen WR, Xiong W, Shepherd GM. Analysis of relations between NMDA receptors and GABA release at olfactory bulb reciprocal synapses. Neuron. 2000; 25:625–633. [PubMed: 10774730]

Clevenger AC, Salcedo E, Jones KR, Restrepo D. BDNF eromoter-mediated -galactosidase expression in the olfactory epithelium and bulb. Chemical Senses. 2008; 33:531–539. [PubMed: 18495654]

Conner JM, Lauterborn JC, Yan Q, Gall CM, Varon S. Distribution of brain-derived neurotrophic factor (BDNF) protein and mRNA in the normal adult rat CNS: evidence for anterograde axonal transport. J Neurosci. 1997; 17:2295–2313. [PubMed: 9065491]

Dahlen JE, Jimenez DA, Gerkin RC, Urban NN. Morphological analysis of activity-reduced adult-born neurons in the mouse olfactory bulb. Front Neurosci. 2011; 5:66.10.3389/fnins.2011.00066 [PubMed: 21602912]

Dean C, Liu H, Staudt T, Stahlberg MA, Vingill S, Buckers J, Kamin D, Engelhardt J, Jackson MB, Hell SW, et al. Distinct subsets of Syt-IV/BDNF vesicles are sorted to axons versus dendrites and recruited to synapses by activity. J Neurosci. 2012; 32:5398–5413. [PubMed: 22514304]

Deckner ML, Frisén J, Verge VM, Hökfelt T, Risling M. Localization of neurotrophin receptors in olfactory epithelium and bulb. Neuroreport. 1993; 5:301–304. [PubMed: 8298092]

Deshpande A, Bergami M, Ghanem A, Conzelmann K-K, Lepier A, Götz M, Berninger B. Retrograde monosynaptic tracing reveals the temporal evolution of inputs onto new neurons in the adult dentate gyrus and olfactory bulb. Proc Natl Acad Sci USA. 2013; 110:E1152–E1161. [PubMed: 23487772]

Diaz D, Lepousez G, Gheusi G, Alonso JR, Lledo PM, Weruaga E. Bone marrow cell transplantation restores olfaction in the degenerated olfactory bulb. J Neurosci. 2012; 32:9053–9058. [PubMed: 22745504]

Edelmann E, Lessmann V, Brigadski T. Pre- and postsynaptic twists in BDNF secretion and action in synaptic plasticity. Neuropharmacol. 2014; 76:610–627.

Egger V, Urban NN. Dynamic connectivity in the mitral cell–granule cell microcircuit. Seminars Cell and Devel Biol. 2006; 17:424–432.

English CN, Vigers AJ, Jones KR. Genetic evidence that brain-derived neurotrophic factor mediates competitive interactions between individual cortical neurons. Proc Natl Acad Sci USA. 2012; 109:19456–19461. [PubMed: 23129644]

Eyre MD, Antal M, Nusser Z. Distinct deep short-axon cell subtypes of the main olfactory bulb provide novel intrabulbar and extrabulbar GABAergic connections. J Neurosci. 2008; 28:8217–8229. [PubMed: 18701684]

Gall CM. Regulation of brain neurotrophin expression by physiological activity. TIPS. 1992; 13:401–403. [PubMed: 1440876]

Gascon E, Vutskits L, Zhang H, Barral-Moran MJ, Kiss PJ, Kiss JZ. Sequential activation of p75 and TrkB is involved in dendritic development of subventricular zone derived neuronal progenitors in vitro. European J Neurosci. 2005; 21:69–80. [PubMed: 15654844]

Gharami K, Xie Y, An JJ, Tonegawa S, Xu B. Brain-derived neurotrophic factor over-expression in the forebrain ameliorates Huntington's disease phenotypes in mice. J Neurochem. 2008; 105:369–379. [PubMed: 18086127]

Glaser EM, Van der Loos H. Analysis of thick brain sections by obverse-reverse computer microscopy: application of a new, high clarity Golgi-Nissl stain. J Neurosci Meth. 1981; 4:117–125.

Gong Q, Bailey MS, Pixley SK, Ennis M, Liu W, Shipley MT. Localization and regulation of low affinity nerve growth factor receptor expression in the rat olfactory system during development and regeneration. J Comp Neurol. 1994; 344:336–348. [PubMed: 8063958]

Gottmann K, Mittmann T, Lessmann V. BDNF signaling in the formation, maturation and plasticity of glutamatergic and GABAergic synapses. Exp Brain Res. 2009; 199:203–234. [PubMed: 19777221]

Gracia-Llanes FJ, Crespo C, Blasco-Ibanez JM, Nacher J, Varea E, Rovira-Esteban L, Martínez-Guijarro FJ. GABAergic basal forebrain afferents innervate selectively GABAergic targets in the main olfactory bulb. Neuroscience. 2010; 170:913–922. [PubMed: 20678549]

Greer C. Golgi analysis of dendritic organization among denervated olfactory bulb granule cells. J Comp Neurol. 1987; 257:442–452. [PubMed: 2435770]

Guthrie KM, Gall C. Anatomic mapping of neuronal odor responses in the developing rat olfactory bulb. J Comp Neurol. 2003; 455:56–71. [PubMed: 12454996]

Guthrie KM, Gall CM. Differential expression of mRNAs for the NGF family of neurotrophic factors in the adult rat central olfactory system. J Comp Neurol. 1991; 313:95–102. [PubMed: 1761757]

Hering H, Sheng M. Dendritic spines: structure, dynamics and regulation. Nat Rev Neurosci. 2001; 2:880–888. [PubMed: 11733795]

Hinds JW, Hinds PL. Synapse formation in the mouse olfactory bulb. I. Quantitative studies. J Comp Neurol. 1976; 169:15–40. [PubMed: 956463]

Hofer M, Pagliusi SR, Hohn A, Leibrock J. Regional distribution of brain-derived neurotrophic factor mRNA in the adult mouse brain. The EMBO Journ. 1990; 9:2459–2464.

Holtmaat AJGD, Trachtenberg JT, Wilbrecht L, Shepherd GM, Zhang X, Knott GW, Svoboda K. Transient and persistent dendritic spines in the neocortex in vivo. Neuron. 2005; 45:279–291. [PubMed: 15664179]

Horch HW, Katz LC. BDNF release from single cells elicits local dendritic growth in nearby neurons. Nature Neurosci. 2002; 5:1177–1184. [PubMed: 12368805]

Huang ZJZ, Kirkwood AA, Pizzorusso TT, Porciatti VV, Morales BB, Bear MFM, Maffei LL, Tonegawa SS. BDNF Regulates the maturation of inhibition and the critical period of plasticity in mouse visual cortex. Cell. 1999; 98:739–755. [PubMed: 10499792]

Imamura F, Greer CA. Dendritic branching of olfactory bulb mitral and tufted cells: regulation by TrkB. PLoS ONE. 2009; 4:e6729.10.1371/journal.pone.0006729 [PubMed: 19707543]

Imayoshi I, Sakamoto M, Ohtsuka T, Kageyama R. Continuous neurogenesis in the adult brain. Devel Growth Differ. 2009; 51:379–386. [PubMed: 19298551]

Isgor C, Sengelaub DR. Effects of neonatal gonadal steroids on adult CA3 pyramidal neuron dendritic morphology and spatial memory in rats. J Neurobiol. 2003; 55:179–190. [PubMed: 12672016]

Jin X, Hu H, Mathers PH, Agmon A. Brain-derived neurotrophic factor mediates activity-dependent dendritic growth in nonpyramidal neocortical interneurons in developing organotypic cultures. J Neurosci. 2003; 23:5662–5673. [PubMed: 12843269]

Kaneko M, Xie Y, An JJ, Stryker MP, Xu B. Dendritic BDNF synthesis is required for late-phase spine maturation and recovery of cortical responses following sensory deprivation. J Neurosci. 2012; 32:4790–4802. [PubMed: 22492034]

Katoh-Semba R, Takeuchi IK, Inaguma Y, Ito H, Kato K. Brain-derived neurotrophic factor, nerve growth and neurotrophin-3 selected regions of the rat brain following kainic acid-induced seizure activity. Neurosci Res. 1999; 35:19–29. [PubMed: 10555160]

Kellner Y, Gödecke N, Dierkes T, Thieme N, Zagrebelsky M, Korte M. The BDNF effects on dendritic spines of mature hippocampal neurons depend on neuronal activity. Front Synaptic Neurosci. 2014; 6 (5):1–17.10.3389/fnsyn.2014.00005 [PubMed: 24478696]

Kelsch W, Lin C-W, Lois C. Sequential development of synapses in dendritic domains during adult neurogenesis. Proc Natl Acad Sci USA. 2008; 105:16803–16808. [PubMed: 18922783]

Kelsch W, Lin CW, Mosley CP, Lois C. A critical period for activity-dependent synaptic development during olfactory bulb adult neurogenesis. J Neurosci. 2009; 29:11852–11858. [PubMed: 19776271]

Kishi K, Mori K, Ojima H. Distribution of local axon collaterals of mitral, displaced mitral, and tufted cells in the rabbit olfactory bulb. J Comp Neurol. 1984; 225:511–526. [PubMed: 6203939]

Knott G, Holtmaat A. Dendritic spine plasticity—Current understanding from in vivo studies. Brain Res Rev. 2008; 58:282–289. [PubMed: 18353441]

Kohara K, Yasuda H, Huang Y, Adachi N, Sohya K, Tsumoto T. A local reduction in cortical GABAergic synapses after a loss of endogenous brain-derived neurotrophic factor, as revealed by single-cell gene knock-out method. J Neurosci. 2007; 27:7234–7244. [PubMed: 17611276]

Kolarow R, Brigadski T, Lessmann V. Postsynaptic secretion of BDNF and NT-3 from hippocampal neurons depends on calcium calmodulin kinase II signaling and proceeds via delayed fusion pore opening. J Neurosci. 2007; 27:10350–10364. [PubMed: 17898207]

Kuczewski N, Porcher C, Gaiarsa J-L. Activity-dependent dendritic secretion of brain-derived neurotrophic factor modulates synaptic plasticity. European J Neurosci. 2010; 32:1239–1244. [PubMed: 20880359]

Laaris N, Puche A, Ennis M. Complementary postsynaptic activity patterns elicited in olfactory bulb by stimulation of mitral/tufted and centrifugal fiber Inputs to granule cells. J Neurophysiol. 2007; 97:296–306. [PubMed: 17035366]

Lepousez G, Nissant A, Bryant AK, Gheusi G, Greer CA, Lledo PM. Olfactory learning promotes input-specific synaptic plasticity in adult-born neurons. Proc Natl Acad Sci USA. 2014; 111:13984–13989. [PubMed: 25189772]

Lessmann V, Brigadski T. Mechanisms, locations, and kinetics of synaptic BDNF secretion: An update. Neurosci Res. 2009; 65:11–22. [PubMed: 19523993]

Luikart BW, Parada LF. Receptor tyrosine kinase B-mediated excitatory synaptogenesis. Prog Brain Res. 2006; 157:15–24. [PubMed: 17167900]

Magby JP, Bi C, Chen ZY, Lee FS, Plummer MR. Single-cell characterization of retrograde signaling by brain-derived neurotrophic factor. J Neurosci. 2006; 26:13531–13536. [PubMed: 17192436]

Matsuda N, Lu H, Fukata Y, Noritake J, Gao H, Mukherjee S, Nemoto T, Fukata M, Poo MM. Differential activity-dependent secretion of brain-derived neurotrophic factor from axon and dendrite. J Neurosci. 2009; 29:14185–14198. [PubMed: 19906967]

Matsumoto T, Rauskolb S, Polack M, Klose J, Kolbeck R, Korte M, Barde Y-A. Biosynthesis and processing of endogenous BDNF: CNS neurons store and secrete BDNF, not pro-BDNF. Nature Neurosci. 2008; 11:131–133. [PubMed: 18204444]

Matsutani S, Yamamoto N. Brain-derived neurotrophic factor induces rapid morphological changes in dendritic spines of olfactory bulb granule cells in cultured slices through the modulation of glutamatergic signaling. Neuroscience. 2004; 123:695–702. [PubMed: 14706781]

Matsutani S, Yamamoto N. Centrifugal innervation of the mammalian olfactory bulb. Anatom Sci International. 2008; 83:218–227.

Matsuzaki M, Honkura N, Ellis-Davies GCR, Kasai H. Structural basis of long-term potentiation in single dendritic spines. Nature. 2004; 429:761–766. [PubMed: 15190253]

McLean JH, Darby-King A, Bonnell WS. Neonatal olfactory sensory deprivation decreases BDNF in the olfactory bulb of the rat. Dev Brain Res. 2001; 128:17–24. [PubMed: 11356258]

Mizoguchi Y, Kanematsu T, Hirata M, Nabekura J. A rapid increase in the total number of cell surface functional GABAa receptors induced by brain-derived Neurotrophic Factor in Rat Visual Cortex. Journal of Biol Chem. 2003; 278:44097–44102. [PubMed: 12941963]

Mizrahi A. Dendritic development and plasticity of adult-born neurons in the mouse olfactory bulb. Nat Neurosci. 2007; 10:444–452. [PubMed: 17369823]

Mizuguchi R, Naritsuka H, Mori K, Yoshihara Y. Tbr2 deficiency in mitral and tufted cells disrupts excitatory-inhibitory balance of neural circuitry in the mouse olfactory bulb. J Neurosci. 2012; 32:8831–8844. [PubMed: 22745484]

Mori K, Nagao H, Yoshihara Y. The olfactory bulb: coding and processing of odor molecule information. Science. 1999; 286:711–715. [PubMed: 10531048]

Nagayama S, Homma R, Imamura F. Neuronal organization of olfactory bulb circuits. Front Neural Circuits. 2014; 8:98.10.3389/fncir.2014.00098 [PubMed: 25232305]

Naritsuka H, Sakai K, Hashikawa T, Mori K, Yamaguchi M. Perisomatic-targeting granule cells in the mouse olfactory bulb. J Comp Neurol. 2009; 515:409–426. [PubMed: 19459218]

Nef SS, Lush MEM, Shipman TET, Parada LFL. Neurotrophins are not required for normal embryonic development of olfactory neurons. Dev Biol. 2001; 234:80–92. [PubMed: 11356021]

Neve RL, Bear MF. Visual experience regulates gene expression in the developing striate cortex. Proc Natl Acad Sci USA. 1989; 86:4781–4784. [PubMed: 2543986]

Néant-Fery M, Pérès E, Nasrallah C, Kessner M, Gribaudo S, Greer C, Didier A, Trembleau A, Caillé I. A role for dendritic translation of CaMKIIα mRNA in olfactory plasticity. PLoS ONE. 2012; 7:e40133.10.1371/journal.pone.0040133 [PubMed: 22768241]

Nissant A, Pallotto M. Integration and maturation of newborn neurons in the adult olfactory bulb - from synapses to function. European J Neurosci. 2011; 33:1069–1077. [PubMed: 21395850]

Orefice LL, Waterhouse EG, Partridge JG, Lalchandani RR, Vicini S, Xu B. Distinct roles for somatically and dendritically synthesized brain-derived neurotrophic factor in morphogenesis of dendritic spines. J Neurosci. 2013; 33:11618–11632. [PubMed: 23843530]

Pallotto M, Nissant A, Fritschy JM, Rudolph U, Sassoe-Pognetto M, Panzanelli P, Lledo PM. Early formation of GABAergic synapses governs the development of adult-born neurons in the olfactory bulb. J Neurosci. 2012; 32:9103–9115. [PubMed: 22745509]

Panzanelli P, Bardy C, Nissant A, Pallotto M, Sassoe-Pognetto M, Lledo PM, Fritschy JM. Early synapse formation in developing interneurons of the adult olfactory bulb. J Neurosci. 2009; 29:15039–15052. [PubMed: 19955355]

Parnass Z, Tashiro A, Yuste R. Analysis of spine morphological plasticity in developing hippocampal pyramidal neurons. Hippocampus. 2000; 10:561–568. [PubMed: 11075826]

Price JL. An autoradiographic study of complementary laminar patterns of termination of afferent fibers to the olfactory cortex. J Comp Neurol. 1973; 150:87–108. [PubMed: 4722147]

Rauskolb S, Zagrebelsky M, Dreznjak A, Deogracias R, Matsumoto T, Wiese S, Erne B, Sendtner M, Schaeren-Wiemers N, Korte M, et al. Global deprivation of brain-derived neurotrophic factor in the CNS reveals an area-specific requirement for dendritic growth. J Neurosci. 2010; 30:1739–1749. [PubMed: 20130183]

Scott JW, McBride RL, Schneider SP. The organization of projections from the olfactory bulb to the piriform cortex and olfactory tubercle in the rat. J Comp Neurol. 1980; 194:519–534. [PubMed: 7451680]

Shepherd GM, Chen WR, Willhite D, Migliore M, Greer CA. The olfactory granule cell: From classical enigma to central role in olfactory processing. Brain Res Rev. 2007; 55:373–382. [PubMed: 17434592]

Shepherd, GM. Olfactory Bulb. In: Shepherd, GM., editor. The Synaptic Organization of the Brain. Oxford University Press; New York: 2004. p. 159-204.

Shieh PB, Ghosh A. Molecular mechanisms underlying activity-dependent regulation of BDNF expression. J Neurobiol. 1999; 41:127–134. [PubMed: 10504200]

Tada T, Sheng M. Molecular mechanisms of dendritic spine morphogenesis. Curr Opinion Neurobiol. 2006; 16:95–101.

Tanaka J-I, Horiike Y, Matsuzaki M, Miyazaki T, Ellis-Davies GC, Kasai H. Protein synthesis and neurotrophin-dependent structural plasticity of single dendritic spines. Science. 2008; 319:1683–1687. [PubMed: 18309046]

Urban NN, Arevian AC. Computing with dendrodendritic synapses in the olfactory bulb. Ann NY Acad Sci. 2009; 1170:264–269. [PubMed: 19686145]

Vigers AJ, Amin DS, Talley-Farnham T, Gorski JA, Xu B, Jones KR. Sustained expression of brain-derived neurotrophic factor is required for maintenance of dendritic spines and normal behavior. Neuroscience. 2012; 212:1–18. [PubMed: 22542678]

Wang, l; Chang, X.; She, L.; Xu, D.; Huang, W.; Poo, M. Autocrine action of BDNF on dendrite development of adult-born hippocampal neurons. J Neurosci. 2015; 35:8384–8393. [PubMed: 26041908]

Whitman MC, Greer CA. Synaptic integration of adult-generated olfactory bulb granule cells: basal axodendritic centrifugal input precedes apical dendrodendritic local circuits. J Neurosci. 2007; 27:9951–9961. [PubMed: 17855609]

Wyatt RM, Tring E, Trachtenberg JT. Pattern and not magnitude of activity determines dendritic spine stability in awake mice. Nature Neurosci. 2012; 15:949–951. [PubMed: 22706266]

Yoshihara Y, De Roo M, Muller D. Dendritic spine formation and stabilization. Curr Opinion Neurobiol. 2009; 19:146–153.

Yoshii A, Constantine-Patton M. Postsynaptic localization of PSD-95 is regulated by all three pathways downstream of TrkB signaling. Front Synaptic Neurosci. 2014; 6(6):1–7.10.3389/fnsyn.2014.00006 [PubMed: 24478696]

Zagrebelsky M, Korte M. Form follows function: BDNF and its involvement in sculpting the function and structure of synapses. Neuropharmacol. 2014; 76:628–638.

Zou D-J, Greer CA, Firestein S. Expression pattern of alphaCaMKII in the mouse main olfactory bulb. J Comp Neurol. 2002; 443:226–236. [PubMed: 11807833]

Research Highlights

- Olfactory granule cells express high levels of BDNF under the CAMKIIa promoter in transgenic mice
- In vivo, BDNF over-expression in granule cells results in increased total spine density
- Increases in spine densities are most pronounced in proximal and outer apical dendritic domains
- Elevated BDNF levels increase the density of mature spines on granule cell apical dendrites

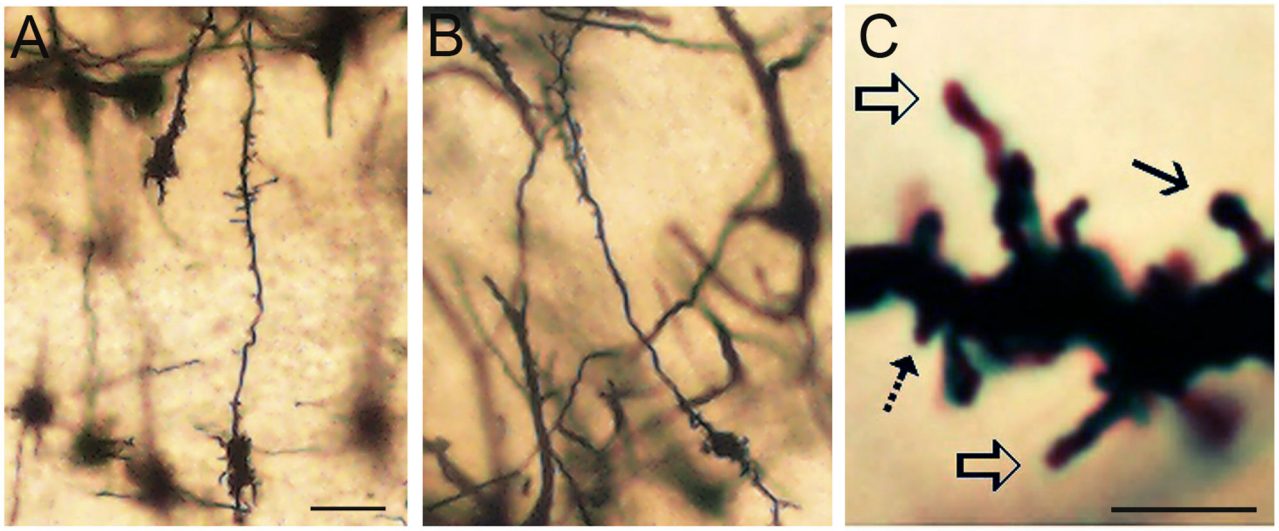

Figure 1.

Photomicrographs showing examples of Golgi-Cox impregnated granule cells bearing dendritic spines (A–B). (C) Proximal apical dendritic segment from a granule cell in a mouse over-expressing BDNF. Arrows indicate the different morphologies of granule cell spines. The solid black arrow indicates an example of a headed spine, the open arrows indicate filopodia, and the dotted arrow indicates a spine classified as other-type. Bar = 10μm in A–B, and 5μm in C.

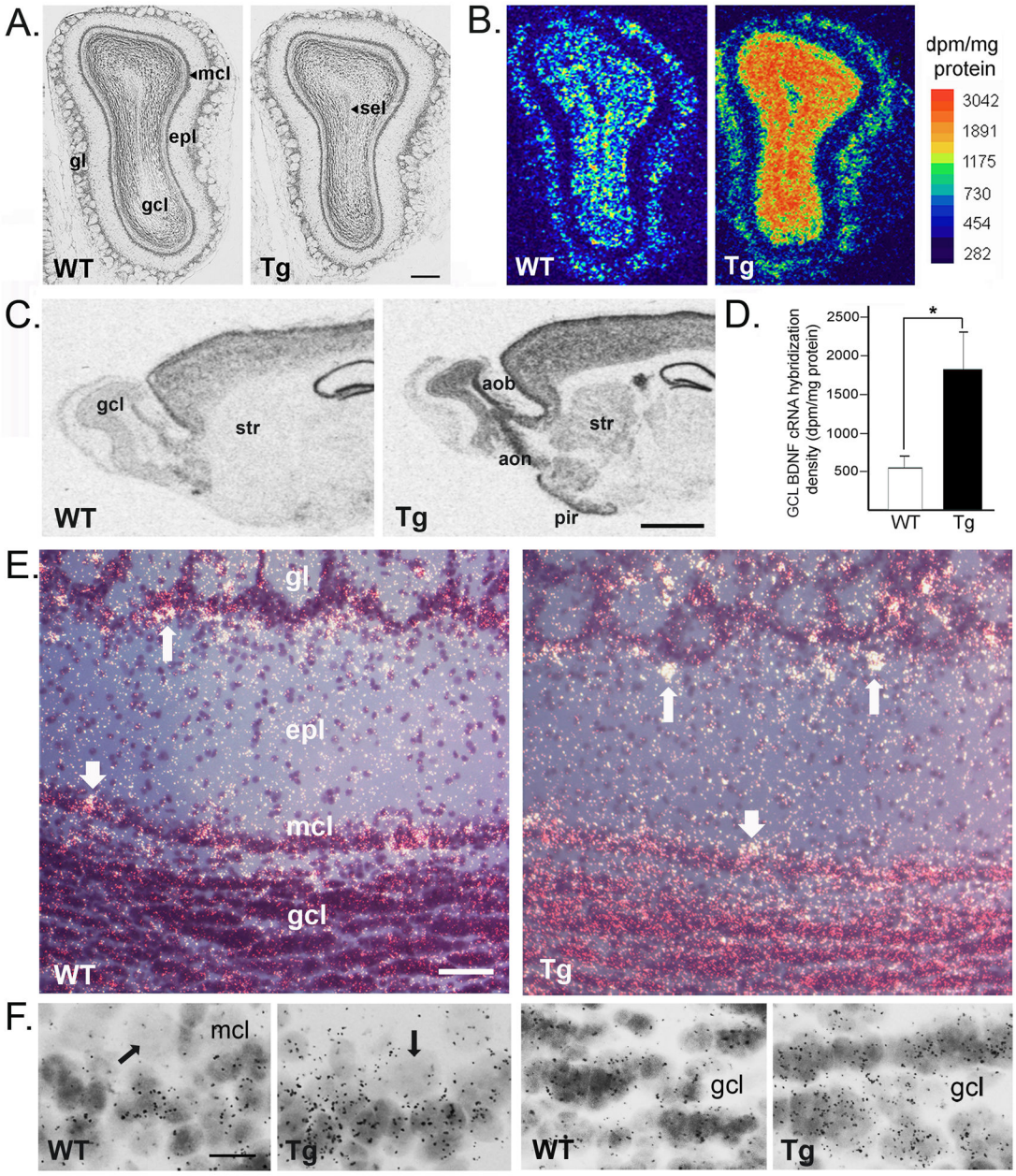

Figure 2.

(A) Nissl-stained coronal sections showing olfactory bulb lamination in a young adult wild-type mouse (WT) and a transgenic mouse (Tg). (B) Calibrated, pseudocolor images of film autoradiograms comparing BDNF cRNA hybridization density in bulb sections from WT and Tg mice. (C) Raw film images of sagittal sections from littermate WT and Tg mice comparing cRNA hybridization in forebrain. In Tg mice, olfactory structures, including the accessory bulb (aob), anterior olfactory nucleus (aon) and piriform cortex (pir) display increased BDNF mRNA expression. The striatum (str), which in normal mice is well known to be devoid of endogenous BDNF mRNA expression, does express BDNF mRNA under control of the CAMKIIα promoter. (D) Levels of BDNF mRNA in the granule cell layer

(gcl) are higher in Tg mice, as quantified by densitometry. Bars indicate group mean values +/− SEM (*p<0.01, unpaired t-test, n=4 per genotype). (E) Dark-field photomicrographs showing cRNA labeling (silver grains are white) in the olfactory bulbs of WT and Tg mice. Labeled cells in the juxtaglomerular region are indicated by long arrows. Thick arrows indicate cells located in or near the mitral cell layer (mcl). (F) Two left panels: High magnification bright-field images of the mitral cell (mcl) and superficial granule cell layers showing that autoradiographic silver grains do not accumulate over mitral cells (arrows indicating large, pale cells) in either WT or Tg mice. Silver grains overly nearby cells in the superficial granule cell layer, with higher grain density seen over cells in the transgenic (Tg) mouse bulb. Two right panels: Scattered silver grains overlying cells in the deep granule cell layer in WT and Tg mice (the subependymal layer is to the bottom in each panel). Cells in the transgenic (Tg) bulb exhibit higher BDNF cRNA-associated grain density. gl, glomerular layer, epl, external plexiform layer; sel, subependymal layer. Bar in A=220μm, in C=1.5mm, in E=100μm, in F=15μm.

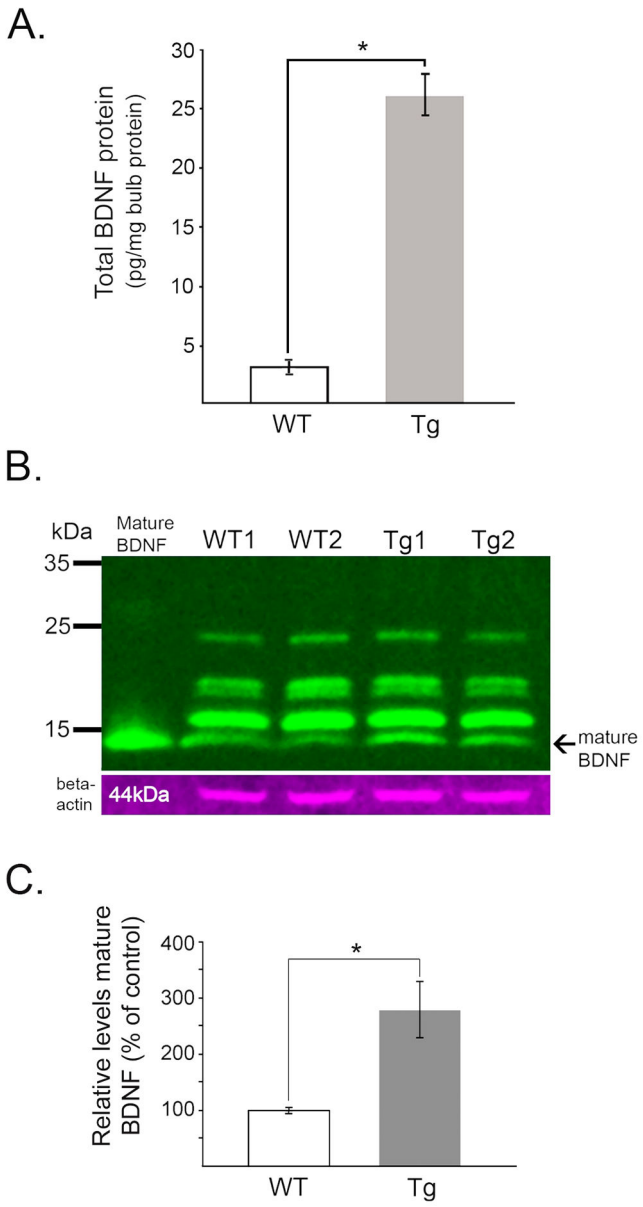

Figure 3.

Olfactory bulbs from adult mice over-expressing BDNF contain higher levels of BDNF protein. (A) ELISA quantification of total bulb BDNF content show significantly higher levels of BDNF in bulbs from adult transgenic (Tg) mice (*p<0.0001; unpaired t-test, n=4 per genotype). (B) Mature BDNF (~14 kDa) was visualized in Western blots of bulb lysates from wild-type (WT) and transgenic mice, with recombinant BDNF peptide (5 ng) as control. This antibody also detects non-specific bands of higher molecular mass. (C) Semi-quantitative measures of mature BDNF (14kDa bands) from Western blots of olfactory bulb lysates. Bar graph shows group mean relative levels +/− SEM (*p<0.05, n=4 per genotype).

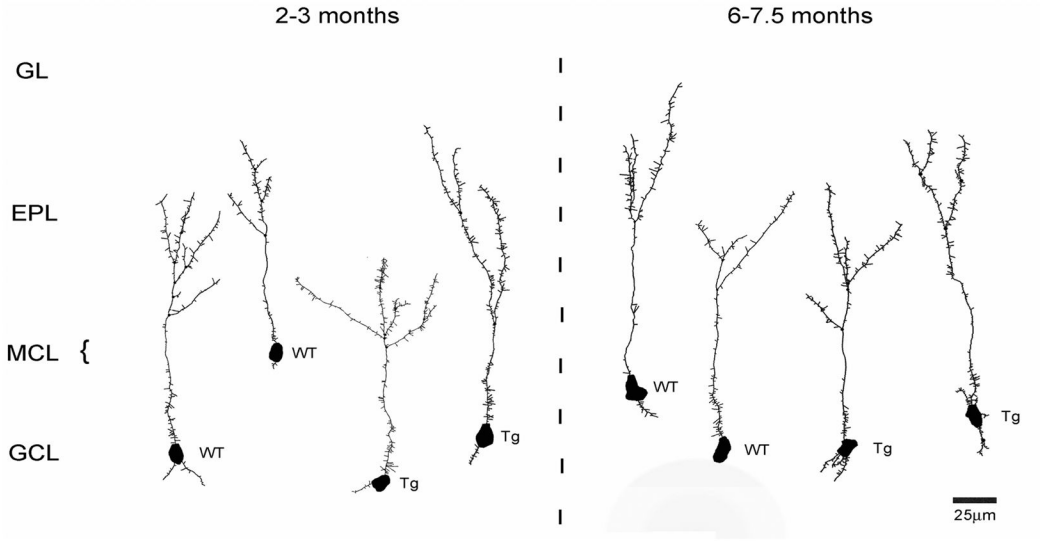

Figure 4.

Representative Neurolucida reconstructions of granule cells from mice of each genotype and age. A total of 178 granule cells were reconstructed. Labels to the left indicate cell location relative to bulb laminae. EPL, external plexiform layer; GL, glomerular layer; GCL, granule cell layer; Tg, transgenic mouse; WT, wild-type control.

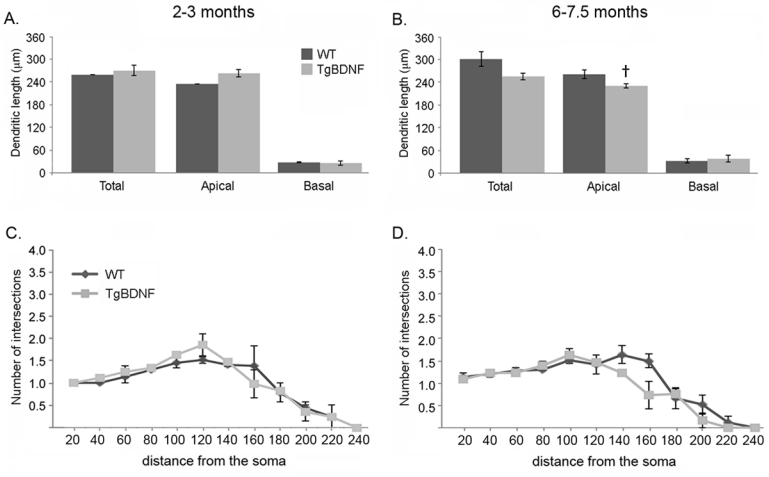

Figure 5.

(A–B) Comparison of granule cell dendritic length in normal and transgenic mice (TgBDNF) at 2–3 months of age (A) and 6–7.5 months of age (B). Total, apical, and basal dendritic lengths show no significant differences between TgBDNF mice and their age-matched, wild-type (WT) controls ($p>0.50$, unpaired t-tests). However, an age difference in apical dendritic length was measured in TgBDNF mice (compare bar in A vs bar in B; $^{\dagger}p<0.05$, unpaired t-test). (C–D) Sholl analysis of mean numbers of GC apical dendritic intersections at 20μm intervals from the cell soma obtained for 2–3 month old mice (C) and 6–7.5 month-old mice (D). No significant genotype-related differences were evident at any distance from the soma ($p>0.05$ for all, unpaired t-tests).

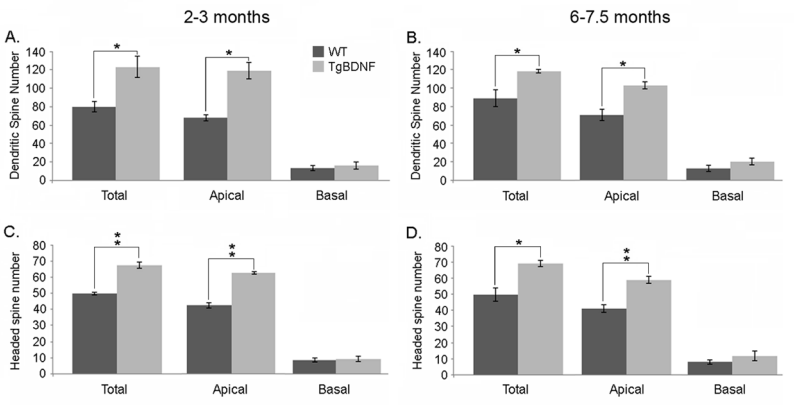

Figure 6.

Analyses of granule cell spine numbers. Bars indicate group mean values +/− SEM (unpaired t-tests). (A–B) TgBDNF mice show a significant increase in total spine number in the apical compartment when compared to age-matched WT mice (*=$p<0.05$, unpaired t-test). (C–D) Headed spine number is also increased in transgenic mice versus controls at both ages (**$p<0.01$, unpaired t test).

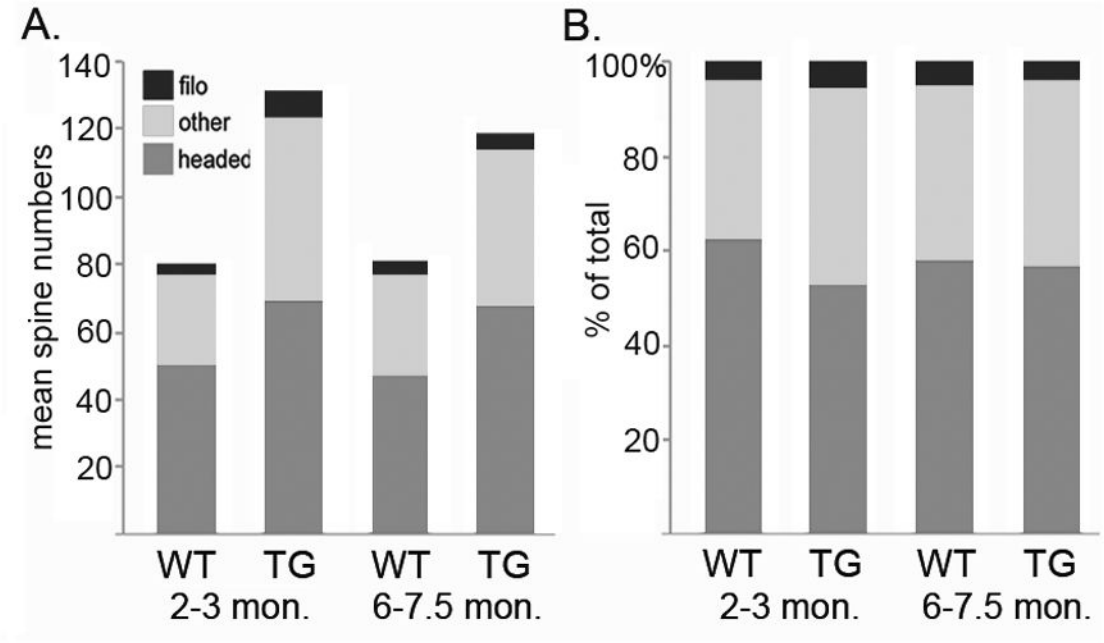

Figure 7.

Bar graphs representing the proportions of different spine types comprising the total numbers for each age and genotype. Group mean values were used.

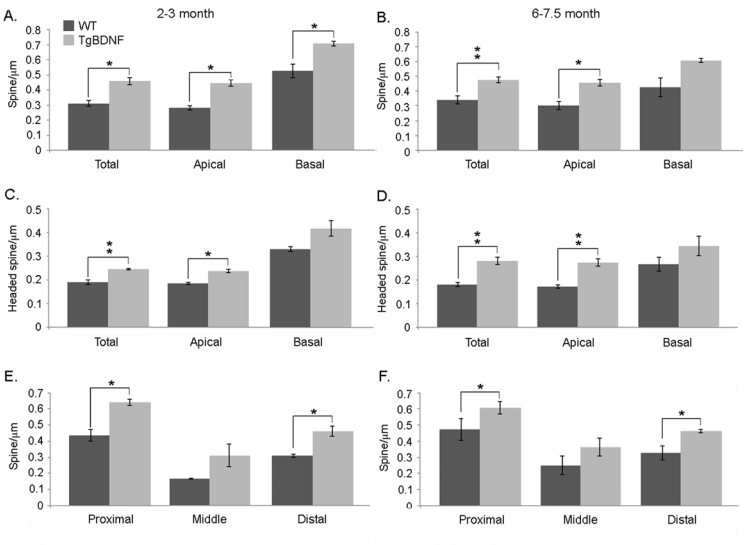

Figure 8.

Analysis of granule cell spine density. Bars indicate group mean values +/− SEM. (A–B) TgBDNF mice show increased spine density in apical and basal dendrites at 2–3 months. In older mice, differences in basal spine density did not reach significance, while apical measures remained significantly higher in transgenic mice. (C–D) Densities of headed spines in TgBDNF mice exceeded measures from WT mice at both ages. (E–F) Measures of apical spine density in the proximal (first 50µm), middle (second 50µm) and distal (dendrite beyond the first 100µm). Proximal and distal spine densities were significantly increased in TgBDNF mice compared to WT controls (*p<0.05, **p<0.01, t-tests).